# Performance of new fringe-detecting avalanche photodiodes at COAST

A. V. George[a], J. E. Baldwin[a], R. C. Boysen[a], C. A. Haniff[a], C. D. Mackay[b], D. Pearson[a], J. Rogers[a], P. J. Warner[a], D. M. A. Wilson[a] and J. S. Young[a]

[a]Astrophysics Group, Cavendish Laboratory, Madingley Road, Cambridge CB3 0HE, UK
[b]Institute of Astronomy, Madingley Road, Cambridge CB3 0HA, UK

## ABSTRACT

At the Cambridge Optical Aperture Synthesis Telescope (COAST), first-generation photon counting avalanche photodiodes (APDs) have been used as the pupil-plane fringe detectors in the optical regime. These are being replaced with EG&G's super-low k ('SliK') APDs, which have an exceptionally low dark count (fewer than 100 counts per second) and high detection efficiency (up to 70% at 700nm). The new detectors have increased the limiting magnitude of the telescope, enabling the observation of targets previously too faint to be seen. We shall discuss the operation of these devices at COAST and present new interferometric observations of stellar objects at visible magnitudes of eight and fainter.

**Keywords:** detectors, optoelectronic devices, avalanche photodiode, APD, photon counting, fringe detection, optical, interferometry

## 1. INTRODUCTION

In the optical (650 nm – 1000 nm) band, COAST uses single pixel photon-counting detectors to measure interference fringes in the pupil plane. The efficiency and noise characteristics of these detectors set a limit on the signal-to noise ratio of our visibility measurements and hence on the faintest magnitude of targets which we can observe.

New fringe-detecting APDs currently being installed at the telescope will allow us to observe targets at I-band magnitudes up to +7, compared with a previous limit of about +5. This will open up new possibilities for science with COAST, including observations in narrow continuum bands on late type stars and measurements of Cepheid diameters at wavelengths below 750 nm.

## 2. THE ROLE OF APDS AT COAST

At COAST, beams from the five separate telescopes are combined in twos (for visibility amplitude measurements) and threes (for closure phase estimation). In either case, the selected beams are first path compensated by movable trolleys on long delay lines, and then passed into the beam combining subsystem. This generates four identical collimated output beams, each containing a quarter of the light from each of the two or three input beams. In order to extract visibility amplitude and closure phase information from the interfered beams, we modulate the path differences between pairs of input beams by moving the delay line trolleys rapidly back and forth during an observation. Thus the interference fringes are realised in the outputs as time-varying intensities. Each of the four outputs is focused onto a single pixel detector which records the photon counts versus time.

Unlike fringe-tracking interferometers, which lock onto a central section of the fringe packet and measure this alone (e.g. NPOI[1]), COAST measures fringes over the entire coherence length of the fringe packet. Large variations in path difference must be introduced in order to scan across the whole packet; in practice, we use a linear scan of 60 μm, which is actually considerably longer then the fringe packet coherence length. This is long enough to keep the fringes within the scan range in spite of atmospheric effects on path difference during the course of an observation, which may last for as long as 100 seconds and consists of a large number of scans back and forth through the fringes. A consequence of the fact that COAST does not fringe track is that its sensitivity is limited by the amount of light required for fringe detection rather than by the (larger) amount of light needed for fringe tracking. (At present COAST's guiding system is more sensitive than the fringe detectors, so this does not limit the telescope's sensitivity.)

Send correspondence to A. V. George (avg20@mrao.cam.ac.uk)

The fringes must be scanned across the output detectors fast enough to ensure that their temporal frequencies do not overlap the atmospheric scintillation spectrum (which extends from very low frequencies to beyond 100 Hz). For visibility amplitude measurements, we use a fringe frequency of around 600 Hz. For closure phase measurements, the measured signal contains fringes on three different baselines instead of just one, and these three sets of fringes must be well separated in frequency space; in practice this means that the highest has to be at around 1500 Hz. The fringe detectors must be read out fast enough to sample this frequency, and so the detectors are typically read out every 0.2 ms during an observation.

## 3. CHOOSING NEW DETECTORS

At COAST we have always used avalanche photodiodes (APDs) as our optical fringe detectors. The first-generation devices were C30902S reach-through silicon APDs, manufactured by EG&G Canada. Each APD was coupled to a 200 μm diameter multimode fibre and incorporated into a custom-designed module containing control electronics and a Peltier cooling system. When they were installed at COAST, these were the only commercially available silicon APDs which could count individual photons. They were chosen above other types of detector, such as p-I-n diodes, photomultipliers and CCDs, because of their high photon detection efficiency (peaking at about 45%), large internal gain, low thermal noise (around 1000 counts/s), lack of readout noise, low cost, robustness and ease of operation[2].

At the present time there is still no other detector which has all of the advantages of APDs for our application. CCDs, with their high quantum efficiency across most of the optical band, are the closest competitors but are as yet ruled out because of their readout noise, which would have to be below the one-electron level to rival the signal to noise ratio given by APDs. During the last few years, however, a number of new photon counting silicon APDs with improved photon detection efficiency and dark count rate have become commercially available. Of these, the super-low k ("SliK") silicon APD manufactured by EG&G Canada combines the highest detection efficiency (peaking at 70% at 700nm) with an exceptionally low dark count rate (fewer than 100 counts/s) and low afterpulsing probability. This device is available as part of a self-contained module (the SPCM-AQ-1XY series) containing control electronics and a cooling system. We will be using these as replacements for COAST's original APD modules. One of these new modules is currently being operated at COAST alongside the remaining three original devices.

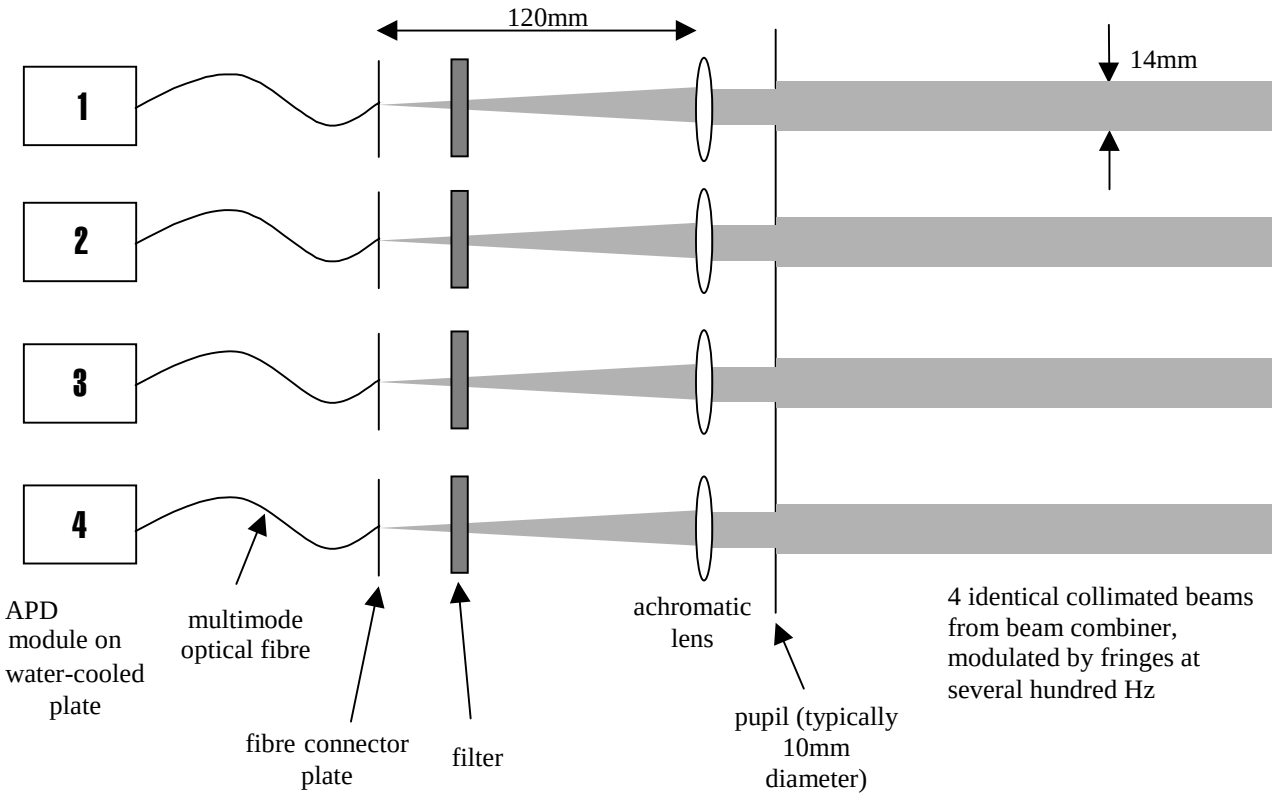


**Figure 1.** Schematic diagram of the optical layout following the beam combiner at COAST.

## 4. PERFORMANCE OF NEW APDS

The new APDs all have dark count rates below 100 cts/s, compared with rates of around 1000 cts/s for our original devices. The detection efficiencies of the modules at several wavelengths were measured at the National Physical Laboratory (the UK's national standards laboratory) using light from a double grating monochromator. Light from the monochromator was imaged onto a circular aperture approximately 50 μm in diameter, and the 100 μm optical fibre feeding the module was mounted with the free end almost in contact with the circular aperture. The detection efficiency was determined by measuring the power exiting from the fibre onto a large area calibrated silicon diode detector (assumed large enough to collect all of the light out of the fibre), and then coupling the fibre into the module and recording the detected counts. By this method the effect of the coupling efficiency into the fibre was eliminated from the measurement. The bandwidth of the radiation used was 6 nm FWHM. The results of these tests are shown in Figure 2, which clearly shows the superiority of the new detectors over the old in terms of efficiency over the whole of COAST's optical wavelength range.

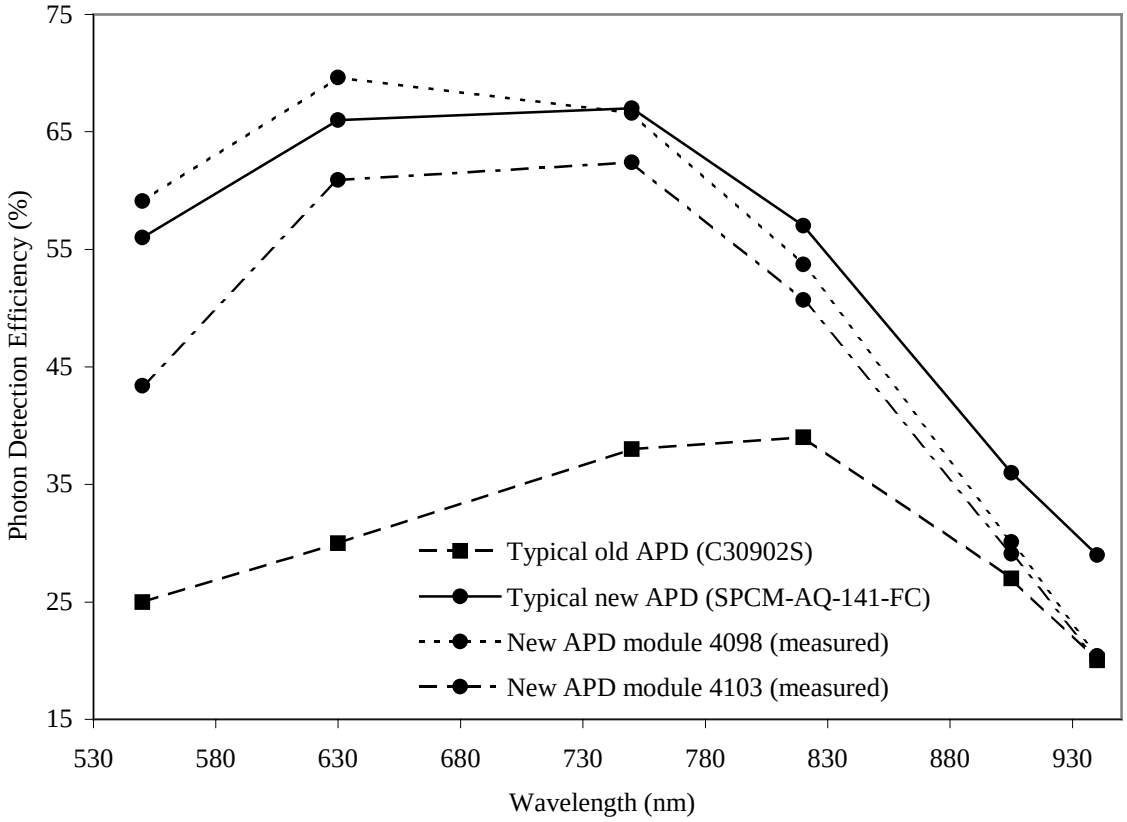


**Figure 2.** Graph showing measured photon detection efficiencies versus wavelength for two of our new APD modules. These measurements were made at the National Physical Laboratory, UK. For comparison, 'typical' curves for both the new modules and our old APDs are also displayed.

## 5. OPERATING NEW APDS AT COAST

We replaced one of our old APD modules along with its optical fibre feed with one of the new modules, to allow direct comparison of the new detector with the remaining three original devices. There are two ways in which light from an output beam out of the beam combiner can fail to reach the detector, and these had to be considered when we installed the new device. First, for an optical fibre there is a maximum incident angle of a light ray into the fibre core for which the ray will be totally internally reflected without loss into the cladding. For the new fibre this angle is 17°. The lowest f/number of a beam which will be completely accepted by the fibre is therefore about 1.7. The f/number of the beam from the fibre lens using the 10 mm pupils is 12, so this condition is easily met for our arrangement. The second potential cause of light wastage is that the beam size at the fibre end may be larger than the fibre core if the beam is not well focused. For our arrangement, with a 100 μm diameter fibre core fed by a beam with f/number 12, the fibre end must be positioned within 0.8 mm of the focal plane if the beam is to be small enough to fit within the core. There are two factors which affect the

position at which the beam from the lens reaches a focus, both of which cause the focus position to vary with observing wavelength. The first is the deviation of the lens from being perfectly achromatic – its focal position actually varies by about 0.5 mm across our observing wavelength range - and the second is the effect of switching filters. At COAST we use a range of filters for different observations across the optical band, and while they all have fairly similar refractive indices, different filters may have thicknesses which differ from each other by as much as 2 mm. Changing between filters can therefore shift the lens focus by up to 1 mm.

To find the position of the lens focus at a given observing wavelength, we use an artificial star to introduce a fixed amount of light into the system. At a certain point along its path, the light from the star is incident on a flat mirror which can be rotated back and forth in azimuth using a motorised mechanism, causing the beam to scan one way and then the other across the fibre end at a regular rate. We simultaneously measure the photon count rates out of the detector. If the beam is well focused at the fibre, it should be small enough to fall entirely within the fibre core. In this case, as the beam sweeps across the fibre, the count rate should rapidly rise from the dark count rate up to a high rate corresponding to the photon counts from the artificial star, and then stay fairly constant as the beam transits the fibre end before falling rapidly when the beam passes off the edge of the fibre. A poorly focused beam may have a larger area than the fibre core, and in this case the count rate rises gradually as the beam passes across the fibre end, reaching a peak before gradually falling again.

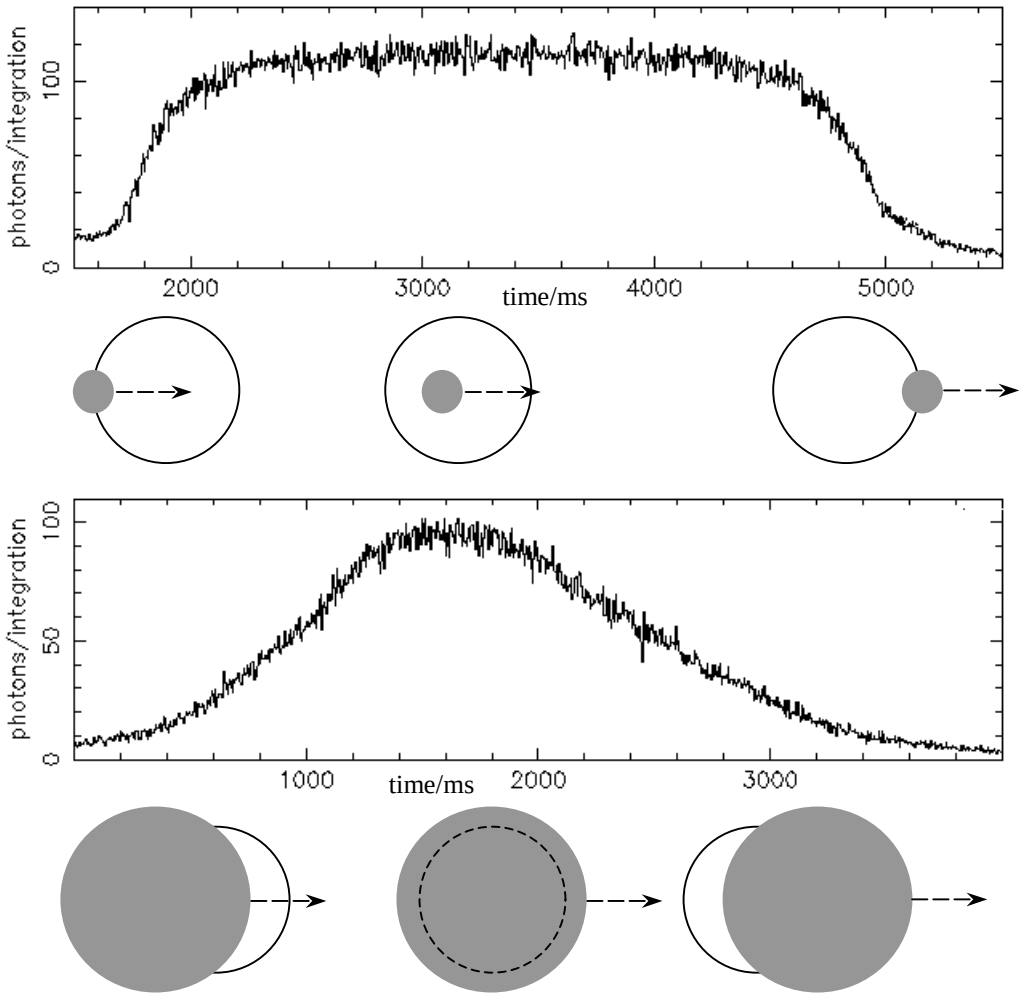


**Figure 3.** Photon counts per 1 ms bin versus time, with beam being scanned across the end of the fibre coupled to the APD. The upper graph shows the results for a well focused beam, while the lower graph shows the results for a poorly focused beam which is larger than the fibre core area. Note that the photon count rate in the upper graph reaches a higher level than the rate in the lower graph, because in the latter case some light spills over the edges of the fibre core and is therefore not detected by the APD. Below each graph are schematic diagrams showing the position of the beam (filled grey circles) relative to the fibre core end (open circles) at different stages in the progress of the beam.

Figure 3 shows two sample measurements of counts (summed over 1 ms bins) versus time. The schematic diagrams below each plot represent stages in the transit of the beam across the fibre end. (The plots are slightly asymmetric, because the motor which rotates a mirror to move the beam is aided by gravity when it moves one way but works against gravity when it moves back, and so runs faster one way than the other.) The upper plot corresponds to a well-focused beam which fits within the fibre core area. In the lower plot, the beam is poorly focused and is slightly larger than the core. Note that in the latter case, the maximum count rate does not reach as high as value as it does in the well-focused case; this is because light in the larger, unfocused beam falls outside the edges of the core and does not reach the APD. It is therefore important to ensure that the beam is always well focused, especially when changing from one observing wavelength to another; we are currently considering an automated scheme for beam focusing.

## 6. OBSERVATIONS

The four APDs were used to measure fringes at 905 nm on the star Lalande 21185, which was first observed by COAST in early 1998[3]. This M dwarf has a V-band magnitude of +7.5 and an I-band magnitude of +5.4 (using the Cousins system of R and I magnitudes[4]), and was the faintest target on which fringes had ever been measured at COAST. Figure 4 shows summed power spectra on Lalande 21185 with one old and one new APD.

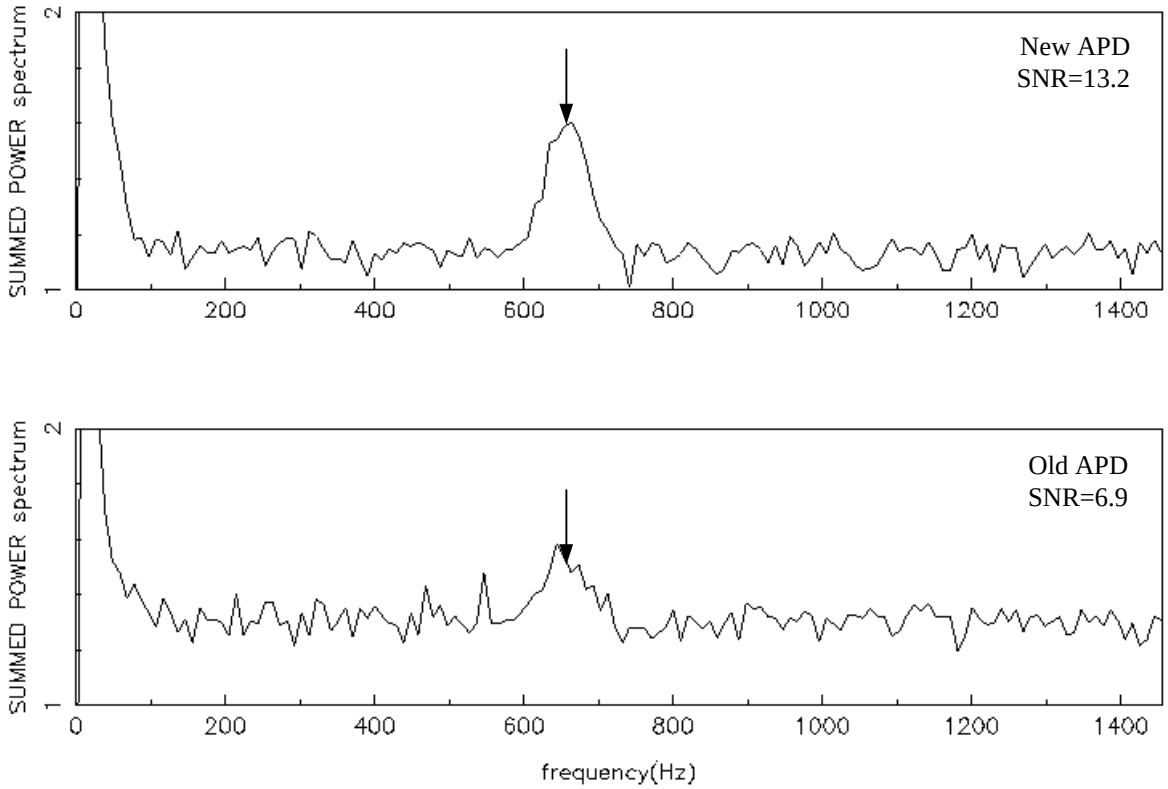


**Figure 4.** Power spectra of fringes measured on Lalande 21185 (I-band magnitude +5.4) at 905 nm at COAST. The upper graph shows data taken with the new APD and the lower graph the old APD. These power spectra were calculated from an observation lasting 100 s, and were produced by incoherently summing the power spectra from each atmospheric coherence time within this 100 s period. We can calculate the expected central fringe frequency from the central observing wavelength and the rate at which the path difference was modulated during the observation, and this frequency is indicated on the graphs by an arrow. The observed signal to noise ratios of the power spectra are marked on the graphs in each case.

Fringes were also recorded on a fainter source, the star HIP 67155, which has a V-band magnitude of +8.5 and an I-band magnitude of +6.4 (again using the Cousins system of R and I magnitudes[4]). This is the faintest object on which we have measured fringes at COAST, and was observed on a night with typical seeing; we estimate that on nights with particularly good seeing we expect to be able to observe targets at I-band magnitudes as faint as +7. As can be seen from the figure, only the new APD was able to detect fringes; with the old detector, the higher dark count level masked the signal.

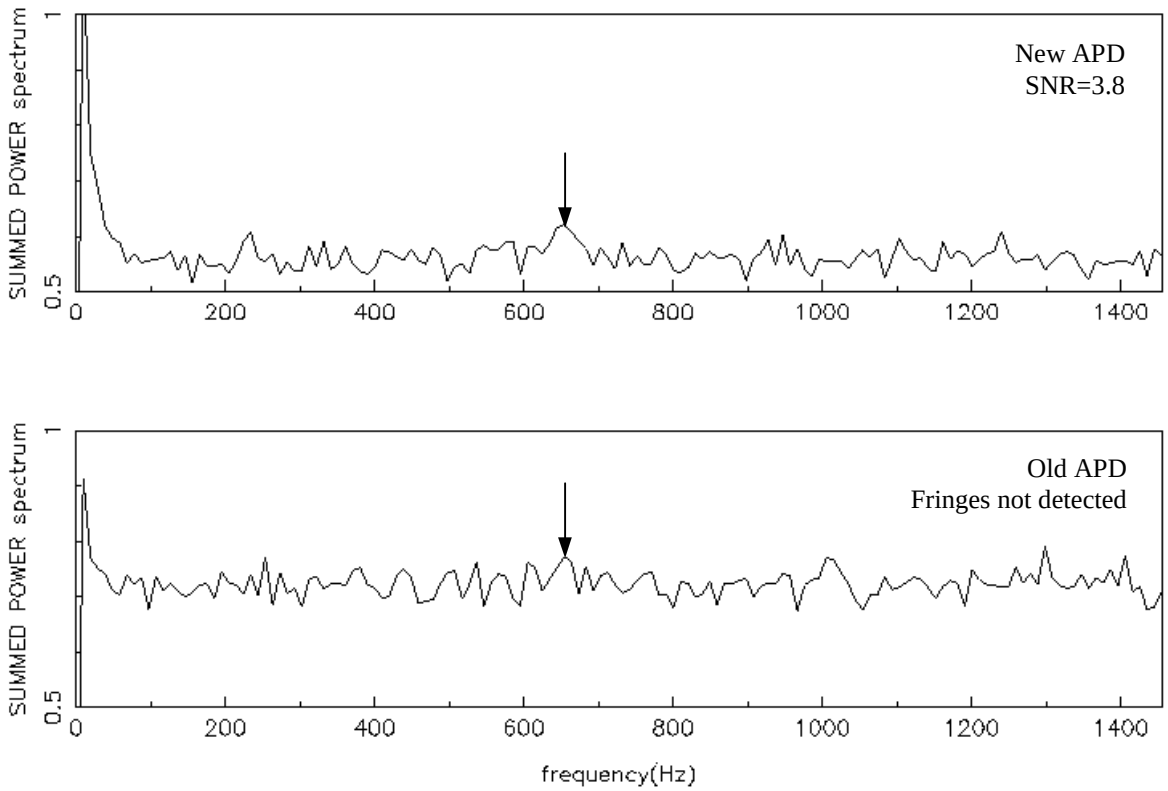


**Figure 5.** Power spectra of fringes measured on HIP 67155 (I-band magnitude +6.4) at 905 nm at COAST. The upper and lower graphs show data taken by the new and old APDs respectively. These power spectra were calculated from an observation lasting 100 s, and were produced by incoherently summing the power spectra from each atmospheric coherence time within this 100 s period. We can calculate the expected central fringe frequency from the central observing wavelength and the rate at which the path difference was modulated during the observation, and this frequency is indicated on the graphs by an arrow. The observed signal to noise ratios of the power spectra are marked on the graphs in each case.

## 7. SIGNAL TO NOISE CALCULATIONS

The theoretical signal to noise ratio of power spectrum measurements made using a detector with thermal noise (a dark count) but no read noise is given by

$$\mathrm{SNR}=\frac{N_{source}^2\eta^2V^2/M^2}{\sqrt{N_{source}^2\eta^2+N_{dark}^2+2N_{source}^3\eta^3V^2/M^2}}$$

where $N_{source}$ is the number of source counts incident on the detector during the observation, $\eta$ is the detector photon detection efficiency at the observing wavelength, $N_{dark}$ is the detector dark count during the observation, V is the observed visibility at the observing wavelength (which is lower than the source's intrinsic visibility owing to degradations caused by the atmosphere and by the imperfect telescope optics), and M is the number of beams being combined at once. (For details of the derivation of this equation see for example Dainty and Greenaway[5].) The three terms in the denominator correspond to Poisson noise from the source counts, Poisson noise from the detector dark counts, and an additional noise term which results from the fact that this is a measurement of the power spectrum rather than the fringe amplitude. Note that this equation only applies over measurement times shorter than the atmospheric coherence time (about 10 ms); in practice we record measurements over the course of many coherence times and incoherently average these to improve the final signal to noise ratio.

Figure 6 shows the signal to noise ratio versus source photon counts of power spectrum measurements taken using the old and new APDs at two different wavelengths, calculated for observed visibility V=0.5 and number of combined beams M=2. Also shown is the signal to noise ratio for an ideal detector with no dark counts and 100% efficiency at all wavelengths.

These graphs are calculated for integrations over a single atmospheric coherence time of 10 ms. In each of the graphs corresponding to the real detectors, there are two main regimes. At low source count values, the dark count term is the dominant noise term in the SNR equation, and the SNR is proportional to $N_{source}^{2}$. At high source counts, the $N_{source}^{3}$ noise term dominates, and the SNR is proportional to $N_{source}^{1/2}$. The location and abruptness of the transition region between these two regimes depend on both the efficiency and the dark count rate of the detector. (The ideal detector graph differs in that at low source counts the dominant noise is the Poisson noise in the source counts, since detector noise is absent.)

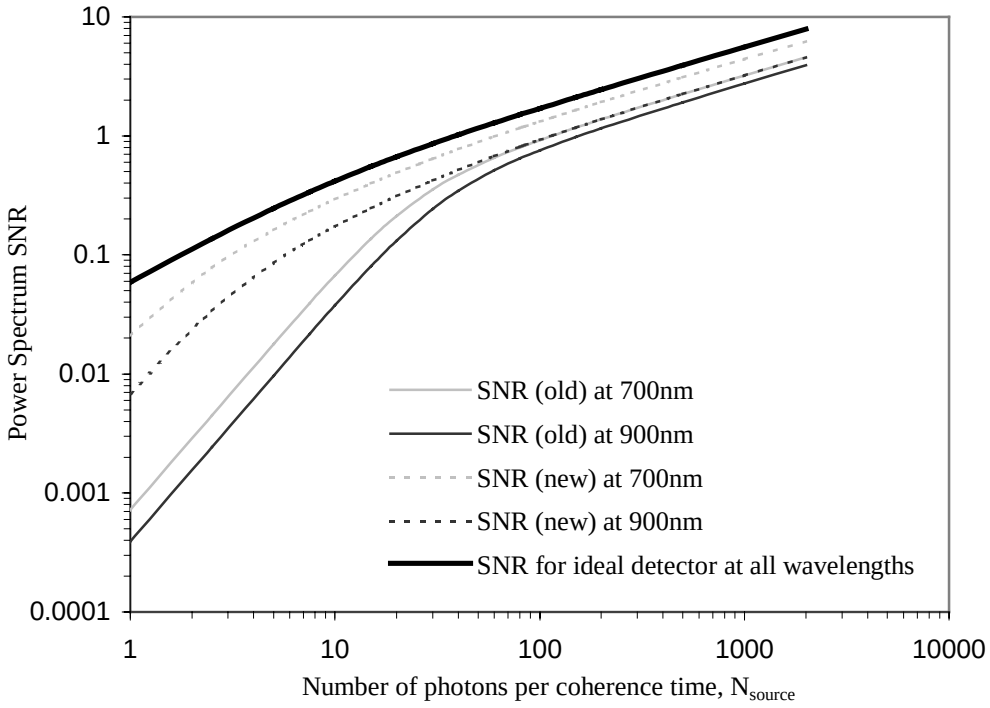


**Figure 6.** Power spectrum signal to noise ratio versus number of source photons for observation over the course of one atmospheric coherence time (10 ms) with the old and new APDs and an ideal detector, at two wavelengths.

## 8. CONCLUSIONS

COAST's limiting magnitude has been substantially improved by the enhanced sensitivity and noise characteristics of the new APD fringe detectors. New areas of science opened up by the improved sensitivity of COAST include:

- observations of Cepheid variables, making use of the high efficiency of the new detectors at short wavelengths at which we can achieve the required resolution for diameter measurement;
- and narrow band continuum measurements (simultaneously using broad band light to locate the fringes) of late type stars.

We have demonstrated that the current-generation photon counting APDs are the best choice for pupil plane fringe detection at COAST in the visible part of the spectrum. These detectors would also be strong candidates for use in future optical interferometers, such as the proposed Large Optical Array[6], where their high detection efficiency and low noise would be crucial factors in determining the capabilities of the instrument.

## 9. REFERENCES

1. J. T. Armstrong, D. Mozurkewich, L. J. Rickard, D. J. Hutter, J.A. Benson, P.F. Bowers, N. M. Elias II, C.A. Hummel, K. J. Johnston, D. F. Buscher, J. H. Clark III, L. Ha, L.-C. Ling, N. M. White and R. S Simon, "The Navy Prototype Interferometer", *Astrophys. J.*, **496**, pp. 550-571, 1998.
2. N. S. Nightingale, "A new silicon avalanche photodiode photon counting detector module for astronomy", *Experimental Astronomy*, 1, pp. 407-422, 1991.

3. J. E. Baldwin, R. C. Boysen, C. A. Haniff, P. R. Lawson, C. D. Mackay, J. Rogers, D. St-Jacques, P.J. Warner, D. M. A. Wilson and J. S. Young, "Current status of COAST", in *Astronomical Interferometry*, R. D. Reasenberg, ed., *Proc. SPIE* **3350**, p. 736, 1998.
4. A. W. J. Cousins, "VRI standards in the E regions", *Mem. R. A. S.* **81**, pp. 25-36, 1976.
5. J. C. Dainty and A. H. Greenaway, "Estimation of spatial power spectra in speckle interferometry", *J. Opt. Soc. Am.* **69**, pp. 786-790, 1979.
6. D. F. Buscher, J. E. Baldwin, R. C. Boysen, A. V. George, C. A. Haniff, D. Pearson, J. Rogers, P. J. Warner, D. M. A. Wilson and J. S. Young, "Technologies for a cost-effective astronomical imaging array", in *Interferometry in Optical Astronomy*, *Proc. SPIE* **4006**, 2000. These proceedings.